Journal of Advanced Research 35 (2022) 245–257

Contents lists available at ScienceDirect

Journal of Advanced Research

journal homepage: www.elsevier.com/locate/jare

Fangchinoline diminishes STAT3 activation by stimulating oxidative stress and targeting SHP-1 protein in multiple myeloma model

Young Yun Jung [a], In Jin Ha [b], Jae-Young Um [a], Gautam Sethi [c,*], Kwang Seok Ahn [a,*]

[a] Department of Science in Korean Medicine, Kyung Hee University, 24 Kyungheedae-ro, Dongdaemun-gu, Seoul 02447, Republic of Korea
[b] Korean Medicine Clinical Trial Center (K-CTC), Korean Medicine Hospital, Kyung Hee University, Seoul 02447, Republic of Korea
[c] Department of Pharmacology, Yong Loo Lin School of Medicine, National University of Singapore, Singapore 117600, Singapore

HIGHLIGHTS

- Aberrant STAT3 activation can promote neoplastic transformation by affecting cellular proliferation, invasion, metastasis, angiogenesis, and anti-apoptosis induction.
- Fangchinoline abrogated protein expression levels of STAT3 and upstream signals (JAK1/2 and Src) in different tumor cells.
- Fangchinoline inhibited the levels of various tumorigenic markers and promoted marked apoptosis through degradation of PARP and caspase-3.
- Fangchinoline attenuated the level of STAT3 and upstream signals and suppressed the level of anti-apoptotic proteins in xenograft mice model.

GRAPHICAL ABSTRACT

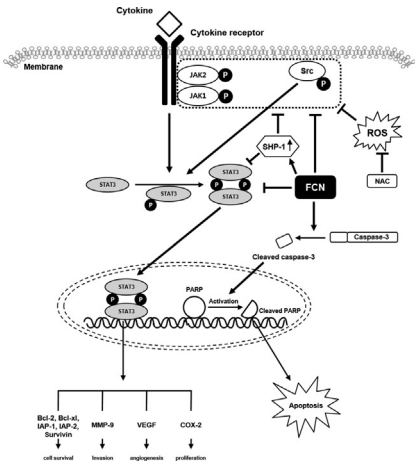

ARTICLE INFO

Article history:
Received 17 October 2020
Revised 15 March 2021
Accepted 16 March 2021
Available online 20 March 2021

Keywords:
Fangchinoline
STAT3
Apoptosis
Multiple myeloma
ROS
GSH

ABSTRACT

Introduction: The development of cancer generally occurs as a result of various deregulated molecular mechanisms affecting the genes that can control normal cellular growth. Signal transducer and activator of transcription 3 (STAT3) pathway, once aberrantly activated can promote carcinogenesis by regulating the transcription of a number of oncogenic genes.
Objectives: Here, we evaluated the impact of fangchinoline (FCN) to attenuate tumor growth and survival through modulation of oncogenic STAT3 signaling pathway using diverse tumor cell lines and a xenograft mouse model.
Methods: To evaluate the action of FCN on STAT3 cascade, protein levels were analyzed by Western blot analysis and electrophoretic mobility shift assay (EMSA). Translocation of STAT3 was detected by immunocytochemistry. Thereafter, FCN-induced ROS was measured by GSH/GSSG assay and H2DCF-DA. FCN-induced apoptosis was analyzed using Western blot analysis and flow cytometry for various assays. Finally, anti-cancer effects of FCN *in vivo* was evaluated in a myeloma model.

Abbreviations: FCN, Fangchinoline; STAT3, signal transducer and activator of transcription 3; SHP-1, Src homology 2 domain-containing protein tyrosine phosphatase-1; c/w, Cell per well; DAPI, 4′,6-Diamidino-2-Phenylindole, Dihydrochloride; FBS, Fetal bovine serum; GAPDH, Glyceraldehyde 3-phosphate dehydrogenase; HRP, Horseradish peroxidase; ICC, Immunocytochemistry; IHC, Immunohistochemistry; ip, Intraperitoneal injection; MMP, Matrix metalloproteinase; DMEM, Dulbecco's Modified Eagle Medium; NT, Non treat; P/S, Penicillin-streptomycin; RTCA, Real-time cell analysis; RT-PCR, Reverse transcription polymerase chain reaction; JAK, Janus kinase; PARP, Poly (ADP-ribose) polymerase; VEGF, vascular endothelial growth factor.

Peer review under responsibility of Cairo University.

* Corresponding authors at: Department of Pharmacology, National University of Singapore, Singapore 129800, Singapore (G. Sethi). Department of Korean Pathology, College of Korean Medicine, Kyung Hee University, 24 Kyungheedae-ro, Dongdaemun-gu, Seoul 02447, Republic of Korea (K.S. Ahn).
E-mail addresses: phcgs@nus.edu.sg (G. Sethi), ksahn@khu.ac.kr (K.S. Ahn).

https://doi.org/10.1016/j.jare.2021.03.008

Results: We noted that FCN abrogated protein expression levels of STAT3 and upstream signals (JAK1/2 and Src). In addition, FCN also attenuated DNA binding ability of STAT3 and its translocation into the nucleus. It altered the levels of upstream signaling proteins, increased SHP-1 levels, and induced substantial apoptosis in U266 cells. FCN also promoted an increased production of reactive oxygen species (ROS) and altered GSSG/GSH ratio in tumor cells. Moreover, FCN effectively abrogated tumor progression and STAT3 activation in a preclinical myeloma model.
Conclusion: Overall, this study suggests that FCN may have a tremendous potential to alter abnormal STAT3 activation and induce cell death in malignant cells along with causing the suppression of pathogenesis and growth of cancer through a pro-oxidant dependent molecular mechanism.

Introduction

Aberrant signal transducer and activator of transcription 3 (STAT3) activation can be found in different malignancies like breast, head and neck, pancreas, prostate cancers, liver, brain, kidney, bladder, and leukemias [1–3]. This transcription factor can promote neoplastic transformation by affecting cellular proliferation, invasion, metastasis, and survival [4–7]. STAT3 can be phosphorylated by upstream kinases JAK1/2 and Src upon stimulation with a plethora of cytokines and growth factors [1,8]. In previous studies, it has been reported that the suppression of aberrant STAT3 phosphorylation by various pharmacological agents can induce apoptosis in tumor cells [3]. In contrast to this STAT3 positive regulation process, diverse tyrosine phosphatases including src homology region 2 domain-containing phosphatase-1, 2 (SHP-1, SHP-2), phosphatase and tensin homolog (PTEN), protein tyrosine phosphatase epsilon (PTPε) etc have been documented to negatively regulate STAT3 activation [9]. Overall, varying studies suggest that blockade of STAT3 signaling can be a key to develop an effective therapeutic approach against human cancers [10–14].

Apoptosis is a programmed cell death process, which is different from other forms like necrosis and autophagy [15,16]. Apoptosis can be controlled by hierarchical molecular sets belonging to *Caenorhabditis elegans* and later in mammalian cells [17–19]. The most representative apoptosis activity markers are poly (ADP-ribose) polymerase (PARP) and caspase-3. Proteolytic cleavage of PARP can alter various events such as transcriptional regulation, DNA repair, and stability. The activation of caspase can be achieved through cleavage, which can promote PARP cleavage into 85- and a 24-kDa fragment [20–23]. Therefore, protein expression analysis of PARP and caspase-3 can play an important role in apoptosis evaluation.

Fangchinoline (FCN) belonging to the family *Menispermaceae* [24–26] can display pleiotropic anti-tumor actions against various transformed cells, causing reduction of cell proliferation and promoting apoptosis [27–30]. In addition, FCN can suppress the AKT phosphorylation, cyclin D1, MMP-2, MMP-9 activation and cause induction of caspase-3 and -8 in osteosarcoma cells [31]. Interestingly, an another study demonstrated that FCN can modulate the focal adhesion kinase (FAK) concomitant with suppression of various oncogenic proteins to repress the invasive activity of tumor cells [32,33].

Oxidative stress can exhibit multifaceted effects on tumor cells. For instance, low levels of reactive oxygen species (ROS) can be beneficial, however, excessive stock of ROS can contribute to tumorigenesis. The production of ROS can be induced intracellularly by mitochondria and other cellular elements, and exogenously by radiation, drugs, pollutants, xenobiotics etc. ROS can also regulate different hallmarks of cancer cells through the modulation of various cell signaling pathways such as STAT3, NF-κB, protein kinases, growth factors, cytokines, hypoxia-inducible factor-1α, and other enzymes [34]. The antioxidant capacity of tumor cells can also aid to remove the excessive ROS to facilitate the resistance to apoptosis and promote survival. However, increased ROS levels in tumor cells can also drive oxidative stress induced-cancer cell death through activating anti-tumorigenic signaling mechanisms [35].

N-acetyl-l-cysteine (NAC) and glutathione (GSH) can also control the process of oxidative stress [36–39]. NAC has been reported to prevent the development of oxidative stress and promote the activation of antioxidant enzymes [39]. The ratio of GSH to oxidized glutathione (GSSG) can indicate the status of oxidative stress within a cell [40]. In this process, glutathione reductase (GR) can catalyze the reduction of GSSG to GSH to repel the process of oxidative stress [41].

In our study, based on the various previously anti-tumor actions of FCN, we deciphered the impact of FCN on STAT3 phosphorylation, which can regulate key hallmarks of cancer. We noted that FCN abolished STAT3 activation in different tumor cells by diverse molecular mechanisms that led to abrogation of tumor growth in a preclinical model. Overall, our findings support the therapeutic development FCN for cancer therapy based on its inhibitory actions on STAT3 activation in tumor cell lines as well as xenograft mouse model.

Materials and Methods

Reagents

Fangchinoline (FCN, Fig. 1A) was purchased from Chem faces (Wuhan, Hubei, China). FCN was stored in 100 mM stock solution with dimethyl sulfoxide at −20 °C and diluted in cultured media for *in vitro* experiments. Tris base, glycine, NaCl, sodium dodecyl sulfate (SDS), and bovine serum albumin (BSA) were purchased from Sigma-Aldrich (St. Louis, MO). Anti-phospho-STAT3 (Tyr705) (9145 s), anti-phospho-JAK1 (Tyr1022/1023) (3331 s), anti-JAK1 (3332 s), anti-phospho-JAK2(Tyr1007/1008) (3776 s), anti-JAK2 (3230 s), anti-phospho-Src(Tyr416) (2101 s), and anti-cleaved-caspase-3 (9661 s) antibodies were obtained from Cell Signaling Technology (Beverly, MA). Anti-STAT3 (sc-8019), anti-Src (sc-5266), anti-Bcl-2 (sc-492), anti-Bcl-xL (sc-7195), anti-Survivin (sc-17779), anti-IAP-1 (sc-7943), anti-IAP-2 (sc-7944), anti-COX-2 (sc-19999), anti-VEGF (sc-7269), anti-MMP-9 (matrix metalloproteinase-9) (sc-393859), anti-caspase-3 (sc-7272), anti-PARP (sc-8007), anti-SHP-1 (sc-287), anti-SHP-2 (sc-280), anti-ki-67 (sc-23900), anti-CD31 (sc-1506) and anti-β-actin (sc-47778) antibodies were purchased from Santa Cruz Biotechnology (Santa Cruz, CA).

Cell lines and culture conditions

Human multiple myeloma (MM) U266, head and neck squamous carcinoma UMSCC 47, non-small-cell lung cancer A549, pancreatic cancer BxPC-3 cells were procured from American Type Culture Collection (Manassas, VA). U266, BxPC-3, and PBMC cells

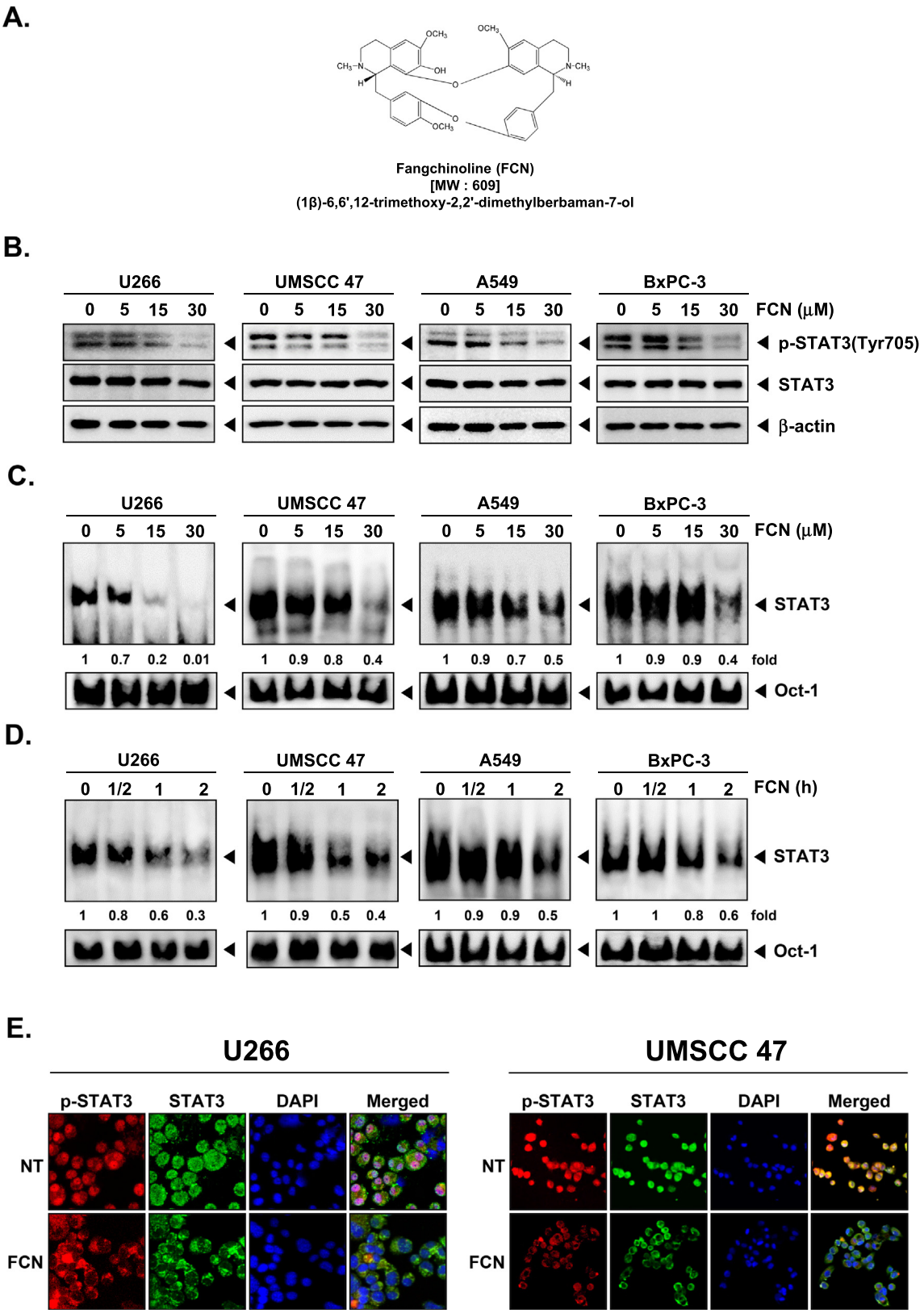

Fig. 1. ***Inhibition of STAT3 phosphorylation by FCN in the neoplastic cells.*** **(A)** The structure of Fangchinoline (FCN). (B) U266, UMSCC47, A549 and BxPC-3 cells were exposed to FCN (0, 5, 15, 30 μM) for 2 h and Western blotting was executed. **(C)** The cells were treated with various concentrations of FCN for 2 h, and nuclear extracts were analyzed by electrophoretic mobility shift assay (EMSA). **(D)** The cells were treated with 30 μM of FCN and STAT3 phosphorylation was studied by Western blot analysis. **(E)** STAT3 translocation activation was observed by immunocytochemistry assay. In U266 and UMSCC47 cells.

were cultured in RPMI-1640 medium containing 10% FBS. UMSCC 47 and A549 cells were grown in DMEM/Low medium containing 10% FBS.

Isolation of human peripheral blood mononuclear cells (PBMCs)

Human peripheral blood mononuclear cells (PBMCs) were isolated from the blood of healthy adult donors (volunteers) via density gradient centrifugation on a Lymphoprep (Axis-Shield PoCAS, Oslo, Norway).

MTT assay

Cells were seeded on 96-well plate and treated with FCN (0, 5, 15, 30 μM) for 24 h. After 24 h of treatment, 30 μl of MTT solution (2 mg/ml) for 2 h, then MTT lysis for overnight. Cell viability was analyzed by measuring absorbance using VARIOSKAN LUX (Thermo Fisher Scientific Inc, Waltham, MA) at 570 nm.

Western blot analysis

Protein expression levels were evaluated by Western blot analysis. Whole cell lysates were extracted from indicated conditions of FCN treated cells. Proteins from cell lysate were prepared with equal amounts to resolved on SDS-PAGE gels and electrotransferred to nitrocellulose membranes. The membranes were blocked using 5% skimmed milk solution (1 × TBST) for 1 h, at room temperature and incubated with primary antibodies for overnight at 4 °C. Thereafter, the membranes were washed by 1 × TBST and incubated with secondary antibodies for 1 h at room temperature. After antibody reaction, membranes were washed again, and detected by enhanced chemiluminescence (ECL) kit (EZ-Western Lumi Femto, DOGEN).

Electrophoretic mobility shift assay (EMSA) for STAT3-DNA binding

To determine whether FCN can suppress the protein-DNA binding reaction, we analyzed U266 cells by EMSA. U266 cells were treated with various concentrations and time conditions of FCN. Nuclei extracts were prepared from whole cell pellets, and incubated with STAT-3 oligonucleotide probe (5′-GATCCTTCTGG GAATTCCTAGATC-3′ and 5′-GATCTAGGAATTCCCAGAAGGATC-3′) and Oct-1 (5′-TTCTAGTGATTTGCATTCGACA-3′ and 5′-TGTCGAATG CAAATCACTAGAA-3′) was used for loading control. Protein-DNA complex was loaded on 5% native polyacrylamid gels and transferred to nylon membrane, then cross-linked by 540 nm UV. Finally, membrane was detected by using LightShift® Chemiluminescent EMSA kit (Waltham, MA).

Real-time cell proliferation analysis

To measure cell growth, first, background impedance was measured in cell culture medium per well. Then cells were seeded on 16 well E-plates, incubated in Roche xCELLigence Real-Time Cell Analyzer (RTCA) DP instrument (Roche Diagnostics GmbH, Germany). FCN (30 μM) treated, then cell index values were measured every 15 min time intervals.

Immunocytochemistry for STAT3 translocation

U266 and UMSCC 47 cells were treated with FCN (30 μM) for 2 h and fixed in 4% paraformaldehyde (PFA) in 1 × PBS for 20 min. The cells were permeabilised by 0.2% Triton X-100 for 10 min, and blocked with 5% BSA in 1 × PBS for 1 h. The cells were probed using anti-p-STAT3 and STAT3 antibodies for overnight at 4 °C, and next day, cells were incubated with secondary antibodies Alexa Fluor® 594 donkey anti-rabbit IgG (H + L) and Alexa Fluor® 488 donkey anti-mouse IgG (H + L) for 1 h at room temperature. Nuclei was probed by 1 μg/ml DAPI for 3 min, used as control. Samples were mounted by Fluorescent Mounting Medium (Golden Bridge International Labs, Mukilteo, WA) and then analyzed by using an Olympus FluoView FV1000 confocal microscope (Tokyo, Japan) [42].

Transfection with electroporation

To knock-down the expression of SHP-1, U266 cells (2×10^6 cells/well) were transfected with SHP-1 and scrambled siRNA (50 nM) for 48 h using by Neon™ Transfection System (Invitrogen, Carlsbad, CA). Cells were collected and resuspended in cultured medium to treated with FCN (30 μM) for 2 or 24 h. Cells were lysied and prepared equal amount of proteins to evaluate the expression of SHP-1, p-STAT3, and PARP by Western blot analysis [43].

Reverse transcription polymerase chain reaction (RT-PCR)

U266 cells were treated with various concentrations of FCN (0, 5, 15, 30 μM) for 2 h. Cells were harvested, suspended in trizol then incubated with chloroform and isopropanol. Extracted RNA was reverse transcribed into cDNA, and examined RT-PCR using superscript reverse transcriptase and Taq polymerase (TAKARA, Tokyo, Japan). For quantitative PCR analyses, Bcl-2 and Bcl-xl were polymerized using the following primers: Bcl-2, 5′-TTGTGGCCTTCTTT GAGTTCGGTG-3′ and 5′-TACAGTTCCACAAAGGCATCCCAG-3′. Bcl-xl, 5′-TACCAGCCTGACCAATATGGC-3′ and 5′-TGGGTTCAAGT GATTCTCCTG-3′. RT-PCR was performed with Bcl-2 at 94 °C for 15 min, 94 °C for 15 sec, 58 °C for 30 sec, 72 °C for 1 min with 28 cycles and extension at 72 °C 5 min. Bcl-xl was performed at 94 °C for 2 min, 94 °C for 30 sec, 57 °C for 30 sec, 72 °C for 1 min with 30 cycles and extension at 72 °C 7 min. Glyceraldehyde-3-phosphate dehydrogenase (GAPDH) was used as control and all experiments were performed at least 3 times individual repeats.

GSH/GSSG assay

U266 cells (1×10^6 cells/well) were treated with FCN (30 μM) for 12 h. Then GSH/GSSG was evaluated according to the described method [44].

ROS detection assay

Intracellular production of ROS was measured using cell-permeable fluorescent 2′,7′-dichlorofluorescin diacetate (H2DCF-DA). U266 cells (1×10^6 cells/well) were treated with FCN (30 μM) for 12 h. After the cells were treated with the indicated conditions, the cells were harvested and washed with PBS. HDF cells were stained with 10 μM H2DCF-DA at 37 °C for 40 min and analyzed with BD Accuri™ C6 Plus Flow Cytometer (BD Biosciences, Becton-Dickinson, Franklin Lakes, NJ) [43].

Mitochondrial membrane potential (MMP) assay

The cells were treated with FCN (30 μM) for 24 h, then harvested to PBS washing. Thereafter they were stained by tetramethylrhodamine ethyl ester (TMRE) with 500 μl PBS in final concentration 50 nM. The cells were than incubated for 30 min, and then analyzed by BD Accuri™ C6 Plus Flow Cytometer (BD Biosciences, Becton-Dickinson, Franklin Lakes, NJ).

Cell cycle analysis

U266 cells (1×10^6 cells/well) were treated with FCN (0, 5, 15, 30 μM) for 24 h and washed with 1 × PBS. The cells were fixed with cold 70% EtOH and incubated overnight at 4 °C. Then fixed cells were washed with 1 × PBS again, and incubated with 1 mg/ml RNase A for 1 h at 37 °C. After 1 h, cells were stained with propidium iodide (PI) and analyzed by BD Accuri™ C6 Plus Flow Cytometer (BD Biosciences, Becton-Dickinson, Franklin Lakes, NJ) with BD Accuri C6 Plus software [2].

Annexin V/TUNEL assays

U266 cells (1×10^6 cells/well) were treated with FCN (0, 5, 15, 30 μM) for 24 h and washed with 1 × PBS. Cells were collected and resuspended in fresh 1 × PBS with FITC tagged Annexin V antibody and PI staining fot 15 min at room temperature. Apoptosis of cells was analyzed by BD Accuri™ C6 Plus Flow Cytometer (BD Biosciences, Becton-Dickinson, Franklin Lakes, NJ) with BD Accuri C6 Plus software [37].

Ethics statement

All experiments involving animals were conducted according to the ethical policies and procedures approved by Kyung Hee University Institutional Animal Care and Use committee [KHUASP (SE)-18–125].

Experimental protocol

Six-week-old athymic nu/nu male mice were purchased form Nara Biotec CO. (Gyeonggi-do, Korea). The mice were randomized into following four treatment groups (n = 5/group) after myeloma has been established by sub-cutaneous injection of U266 cells. Group I, control, was treated with PBS (100 μl; i.p.; 3 times/week), group II was treated with FCN (2.5 mg/kg; i.p.; 3 times/week), group III was treated with FCN (5 mg/kg; i.p.; once a week. Therapy was continued for 20 days from the randomization (Day 0). Mice were killed 5 days later after the last therapy and processed as described earlier.

Western blot and immunohistochemical analysis

These assays were executed on tumor tissues as described previously [45].

Statistical analysis

All the numerical values have been represented as the mean ± SD. Statistical significance of the data compared with the untreated control was determined using the Student unpaired t-test, Sigmaplot 10.0 (USA, Canada). Significance was set at $^*P < 0.05$, $^{**}P < 0.01$, and $^{***}P < 0.001$.

Results

FCN suppresses STAT3 phosphorylation in tumor cells

To confirm impact of FCN on STAT3 phosphorylation, we first evaluated phospho-STAT3 expression level in various cell lines, namely U266, UMSCC 47, A549, and BxPC-3 (Fig. 1B). The results showed that FCN exerted a substantial suppressive effects on STAT3 phosphorylation, but had no effects on total STAT3 expression. Then we deciphered the actions of FCN on STAT3-DNA binding activity and noticed that it was attenuated in both concentration and time-dependent fashion (Fig. 1C and D). Based on the above results, we selected U266 cells and UMSCC 47 cells, which were most responsive to FCN exposure, to confirm its impact on the nuclear translocation of STAT3. In both U266 and UMSCC 47 cells, it was clearly observed that the expression of p-STAT3 and STAT3 in the cells treated with FCN was localized predominantly in the cytoplasm rather than in the nucleus (Fig. 1E). The phosphorylated STAT3 monomers can undergo dimerization and move into nucleus to drive the expression of target genes. Since there was a significant reduction in the phosphorylation of STAT3, a decline in the nuclear pool of STAT3 can also be expected. Thus, FCN was identified to target STAT3 activation cascade at different molecular levels.

FCN alters the levels of STAT3 regulatory proteins

Because STAT3 can be regulated by different upstream signals [46], we confirmed the impact of FCN on JAK1/2 and Src phosphorylation. As shown, FCN exhibited a pronounced suppressive effects on phosphorylation of STAT3 upstream signals JAK1/2 and Src kinases (Fig. 2A). Thereafter, we evaluated the effects of FCN on SHP-1 and SHP-2 proteins which can act as major negative regulators of STAT3 phosphorylation in U266, UMSCC47, A549, and BxPC-3 cells. As depicted, FCN exposure only induced the levels of SHP-1 protein (Fig. 2B). According to these results, we focused primarily on U266 cells which expressed highest levels of SHP-1 protein for detailed analysis. Thereafter, phospho-STAT3 expression level was analyzed by Western blotting after pervanadate treatment (Fig. 2C). As protein tyrosine phosphatases have been reported to modulate in STAT3 activation, we also deciphered whether FCN mediated inhibition of STAT3 tyrosine phosphorylation could be caused by activation of a protein tyrosine phosphatase. We confirmed that treatment of U266 cells with protein tyrosine phosphatases inhibitor sodium pervanadate abolished FCN-promoted inhibition of STAT3 activation. It was noted that as the concentration of pervanadate increased, the expression of STAT3 phosphorylation was also noted to increase even in the presence of FCN. Next, we investigated the potential changes that may occur in STAT3 phosphorylation upon gene silencing of *SHP-1*. The results suggested that SHP-1 siRNA induced *SHP-1* gene silencing, and it promoted an increase of phospho-STAT3 protein expression levels in FCN treated cells (Fig. 2D and E).

FCN affects ROS activation in U266 cells

The balance of GSH to oxidized glutathione (GSSG) can regulate the oxidative stress. The ratio of GSH to oxidized glutathione (GSSG) can function as a potential marker of oxidative stress [40]. As shown in Fig. 2F, FCN significantly reduced GSH levels in tumor cells. In addition, GSSG and GSSG/GSH ratio was increased in U266 cells, thereby demonstrating that FCN can induce oxidative stress. Additionally, FCN enhanced the level of ROS in U266 cells as analyzed by flow cytometry analysis (Fig. 2G). N-acetyl-l-cysteine (NAC) is an important regulator of oxidative stress as antioxidant [39], and pre-treatment of NAC was observed to cause recovery of STAT3 abrogation promoted by FCN (Fig. 2H and I). However, NAC treatment reduced the expression of SHP-1 protein level to a great extent in U266 cells (Fig. 2 H)

FCN suppresses tumorigenesis with apoptosis induction

We next investigated whether FCN exhibited greater cytotoxicity in cancer cells as compared to the normal PBMC cells. Interestingly, it was observed that FCN displayed greater cytotoxicity against cancer cells as compared to the PBMC cells (Fig. 3A). Additionally, by using mitochondrial potential assay (MMP assay), we

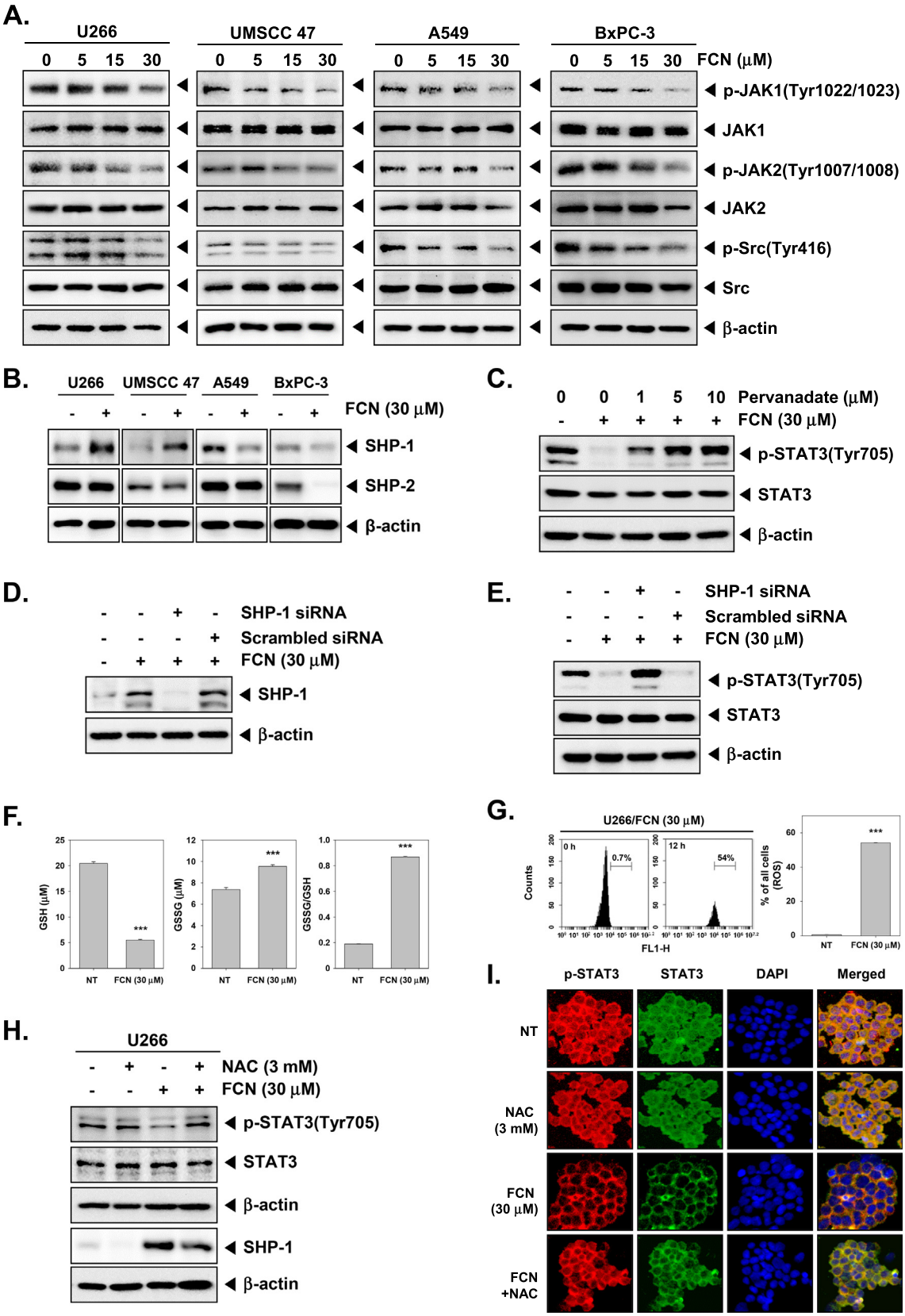

Fig. 2. ***Regulation of STAT3 related signals and ROS by FCN.*** **(A)** U266, UMSCC47, A549, and BxPC-3 cells were treated with FCN (0, 5, 15, 30 μM) for 2 h and western blotting was executed. **(B)** The various human cancer cells, were exposed to FCN and then Src homology region 2 domain-containing phosphatase-1 and 2 (SHP-1 and SHP-2) levels were analyzed. **(C)** U266 cells were pre-treated with pervanadate (0, 1, 5, 10 μM) for 30 min, then incubated with FCN (30 μM) for 2 h and western blotting was executed. **(D and E)** SHP-1 gene silencing by siRNA was carried out followed by western blotting to probe the levels of protein. **(F and G)** U266 cells were treated with FCN (30 μM) for 12 h. Then reactive oxygen species (ROS) suppression by FCN was analyzed by Glutathione/Oxidized glutathione (GSH/GSSG) and oxidative stress assays. **(H)** U266 cells were pre-treated with N-acetyl-cysteine (NAC) (3 mM) for 15 min, then incubated with FCN (30 μM) and Western blot analysis was executed. (I) U266 cells were pre-treated with NAC (3 mM) for 15 min, then treated with FCN (30 μM) for 2 h. Expression of p-STAT3 and STAT3 were evaluated by immunocytochemistry.

evaluated the alterations in the mitochondrial function upon FCN exposure as this function is an important indicator of cellular health [47]. FCN was observed to effectively suppress or cell proliferation (Fig. 3B) and also modulate MMP, as measured by flow cytometry (Fig. 3C). On the contrary, apoptosis, programmed cell death signals were effectively induced by FCN. Caspase-3 and PARP cleavage are considered as well-known apoptosis markers and FCN promoted a robust expression of cleaved forms of both these proteins (Fig. 3D).

FCN increases apoptosis through suppression of levels of tumorigenic proteins

Because FCN-induced caspase and PARP cleavage was noted to be substantial in U266 cells, we representatively investigated the detailed apoptosis activity of the drug in these cells. First, we demonstrated the effects of FCN on different anti-apoptotic proteins at both transcriptional and translational levels. The levels of distinct tumorigenic proteins was decreased as FCN concentration increased (Fig, 4A and B). In addition, we selected Bcl-2 and Bcl-xl which showed a maximal decrease and confirmed the alteration also at RNA expression levels (Fig. 4C). Thereafter, apoptosis activation was analyzed by cell cycle assay and annexin V assays. In Fig. 4D, cell cycle was arrested and stacked in sub G1 phase upon FCN treatment (Fig. 4D). Moreover, FCN caused a marked increase in both early and late apoptosis ratio, however, SHP-1 knock-down using si-RNA could substantially decrease apoptosis induction (Fig. 4F–G).

NAC reduces the FCN-induced apoptosis activations in U266 cells

We next investigated the possible interaction between oxidative stress and apoptosis. U266 cells were pre-treated with NAC (3 mM) for 15 min, and then additionally incubated with FCN (30 μM) for 24 h. To evaluate the apoptotic cell death, protein expression level of PARP was analyzed by Western blot analysis. The results indicated that FCN increased the PARP cleavage, however, NAC reduced it substantially (Fig. 4H). Additionally, as shown on Fig. 4I, FCN induced cell cycle arrest, and the cells were stacked in sub G1 phase. However, treatment of NAC reduced these changes. In Fig. 4J, apoptotic cells were identified by annexin V assay. As shown, FCN exposure increased the percentage of cells undergoing late apoptosis. However, NAC treatment reduced the FCN-induced apoptotic cells significantly.

FCN attenuates tumor progression in a MM preclinical model

To examine the *in vivo* efficacy of FCN, a MM xenograft mouse model was used as per the experimental protocol specified in Fig. 5A. We noticed that tumor volume sharply increased in vehicle group, however, in FCN treated groups it was markedly suppressed (Fig. 5C). Interestingly, tumor weight was also decreased remarkably without significant decrease in normal body weight in FCN treated mice (Fig. 5D and E).

FCN alters the levels of oncogenic biomarkers in tumor tissues

We further evaluated the levels of various oncogenic markers in U266 tumor tissues. As depicted in Fig. 6A, expression of phospho-STAT3, Ki-67, and CD31 was significantly decreased in tumor tissues obtained from treated group. Moreover, protein levels of STAT3 and upstream signals JAK1/2 and Src phosphorylation (Fig. 6C). as well as oncogenic proteins (Bcl-2, Bcl-xl, survivin, IAP-1, IAP-2, COX-2, VEGF, and MMP-9) were clearly attenuated (Fig. 6D) but, the expression of SHP-1, cleaved caspase-3, and cleaved PARP proteins were increased upon FCN exposure (Fig. 6B and E), thus indicating that it can modulate key hallmarks implicated in tumor progression and survival.

Discussion

Persistent activation of STAT3 has been implicated as pivotal molecule involved in the development and differentiation of tumor cells [1–3]. Since the abnormally excessive activity of STAT3 can mediate abnormal proliferation, metastasis, angiogenesis and anti-apoptotic processes, we have evaluated the impact of FCN on STAT3 phosphorylation in various cancer cells. FCN inhibited STAT3 phosphorylation in U266, UMSCC 47, A549, and BxPC-3 cells, as well as affected DNA binding activity and intracellular migration of STAT3. STAT3 can be activated by stimulation with the upstream kinases like JAK1 / 2 and Src [1,8], however, FCN abrogated the levels of these proteins and increased the SHP-1 expression, which is a protein phosphatase and can negatively regulate STAT3 activity [9]. Thus anti-neoplastic actions of FCN may be mediated by altering STAT3 activation at different levels in the signaling cascade.

GSH/GSSG system can function as a robust intracellular antioxidant system, and thus we investigated whether the ratio of GSH/GSSG can also be affected by FCN [48]. Interestingly, FCN decreased the GSH ratio, however, percentage of GSSG was significantly increased in U266 cells. Thereafter exposure of FCN to U266 cells caused a substantial disturbance in the GSH/GSSG system thus indicating that the drug can induce oxidative stress. In addition, FCN significantly increased ROS levels and these results demonstrate that oxidative stress may significantly regulate the diverse anticancer actions of FCN including its STAT3 modulatory effects.

N-acetyl-l-cysteine (NAC), was found to also regulate the oxidative stress process modulating STAT3 phosphorylation. We noticed that NAC treatment reduced the SHP-1 expression, however, FCN could recover the SHP-1 level to great extent. Additionally, NAC decreased the FCN-promoting apoptosis through PARP, cell and the cycle arrest in U266 cells. Overall, the results suggested that NAC could increase the phosphorylation of STAT3 while reducing SHP-1 level and apoptosis induction.

Since apoptosis is one of the important systemic anti-cancer processes in the body, we also studied the FCN-induced apoptotic effects in detail [15,16]. Using MMP assay, we also analyzed the changes of MMP in different cancer cells. Interestingly, in U266, UMSCC 47, A549, and BxPC-3 cells, MMP level was found to significantly decrease upon FCN treatment. FCN also inhibited the levels of various tumorigenic markers and promoted marked apoptosis through degradation of PARP and caspase-3 [20–23]. Additionally, FCN repressed cellular differentiation and growth by causing cell cycle arrest. Moreover, FCN effectively mitigated the levels of various multi-faceted proteins that can control survival (Bcl-2, Bcl-xl, Survivin, IAP-1, IAP-2), proliferation (COX-2), angiogenesis (VEGF), and invasion (MMP9). In addition, FCN can cause a robust arrest of tumor cells in Sub- G1 phase, and induced apoptosis, especially causing the cells to accumulate in late apoptosis phase. These observations are partially in accord with our prior study in which FCN was noted to enhance TNF-driven apoptosis in tumor cells by affecting the levels of NF-κB and AP-1 transcription factors [30].

Finally, by using a preclinical myeloma model, we also elegantly demonstrate that FCN treatment can remarkably reduce tumor size and weight, but loss of mouse body weight was not noted, thereby indicating potential non-toxic nature of the drug. The tumor tissues were also harvested from mice and analyzed for levels of various anticancer biomarkers using different techniques. FCN attenuated the level of STAT3 and upstream signals and suppressed the level of anti-apoptotic proteins in tumor tissues. Moreover, an increase of STAT3 negative regulatory factor, SHP-1, protein

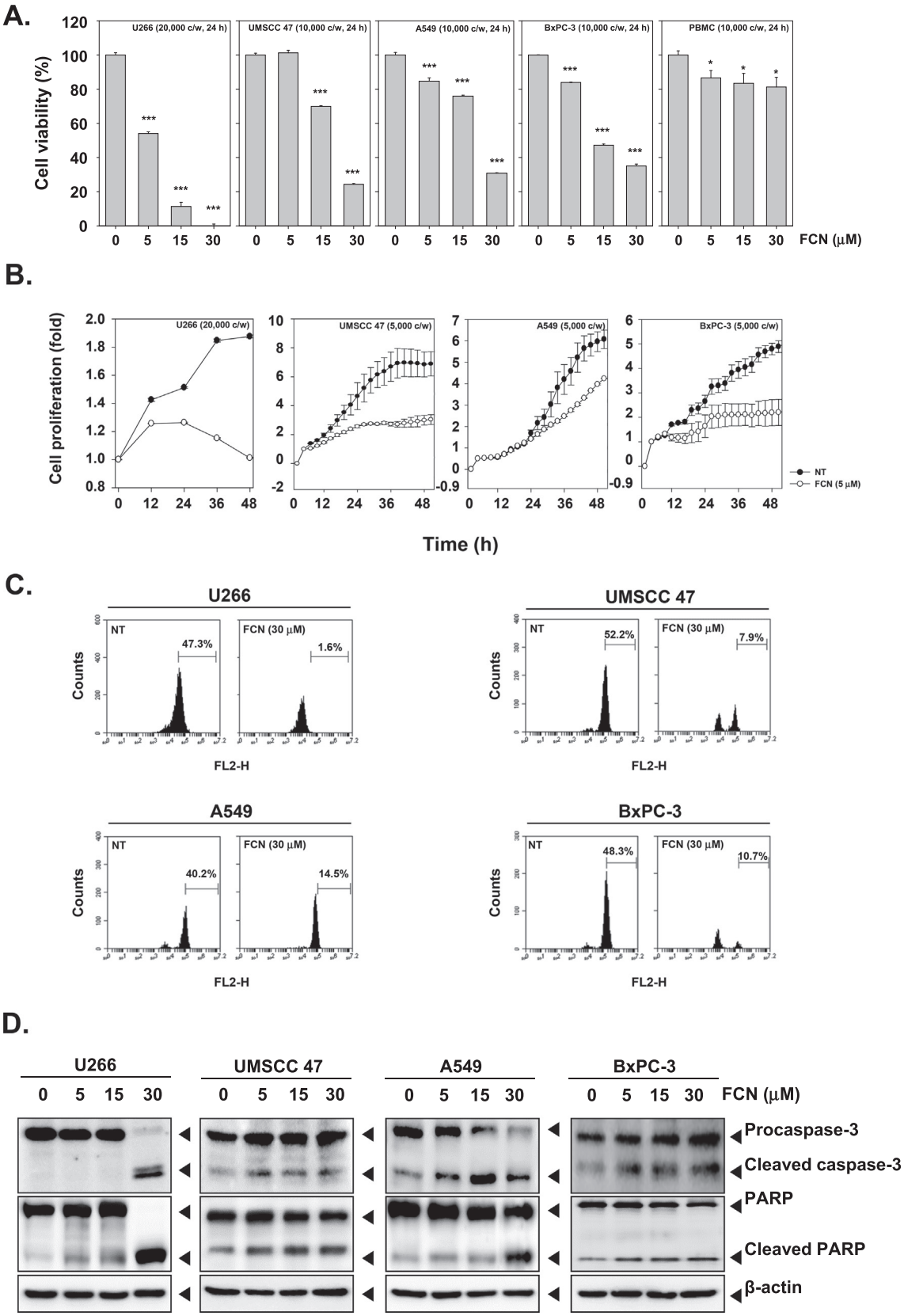

Fig. 3. ***Suppression of tumorigenesis through apoptosis induction by FCN.*** **(A)** U266, UMSCC47, A549, BxPC-3 and peripheral blood mononuclear cell (PBMC) were treated with FCN (0, 5, 15, 30), then cell viability was measured by MTT assay. **(B)** The cells were treated with FCN (30 μM) and proliferation was measured by MTT or real time cell analysis (RTCA). **(C)** FCN-induced apoptosis was analyzed using changes in matrix metalloproteinase (MMP) levels. U266, UMSCC47, A549, and BxPC-3 cells were treated with FCN (30 μM) for 24 h. Then tetramethylrhodamine ethyl ester (TMRE) probed cells were sorted by BD Accuri™ C6 Plus Flow Cytometer. **(D)** Cells were treated with FCN (30 μM) for 24 h and Western blot was executed. Apoptosis activation was evaluated by caspase and PARP cleavage activation.

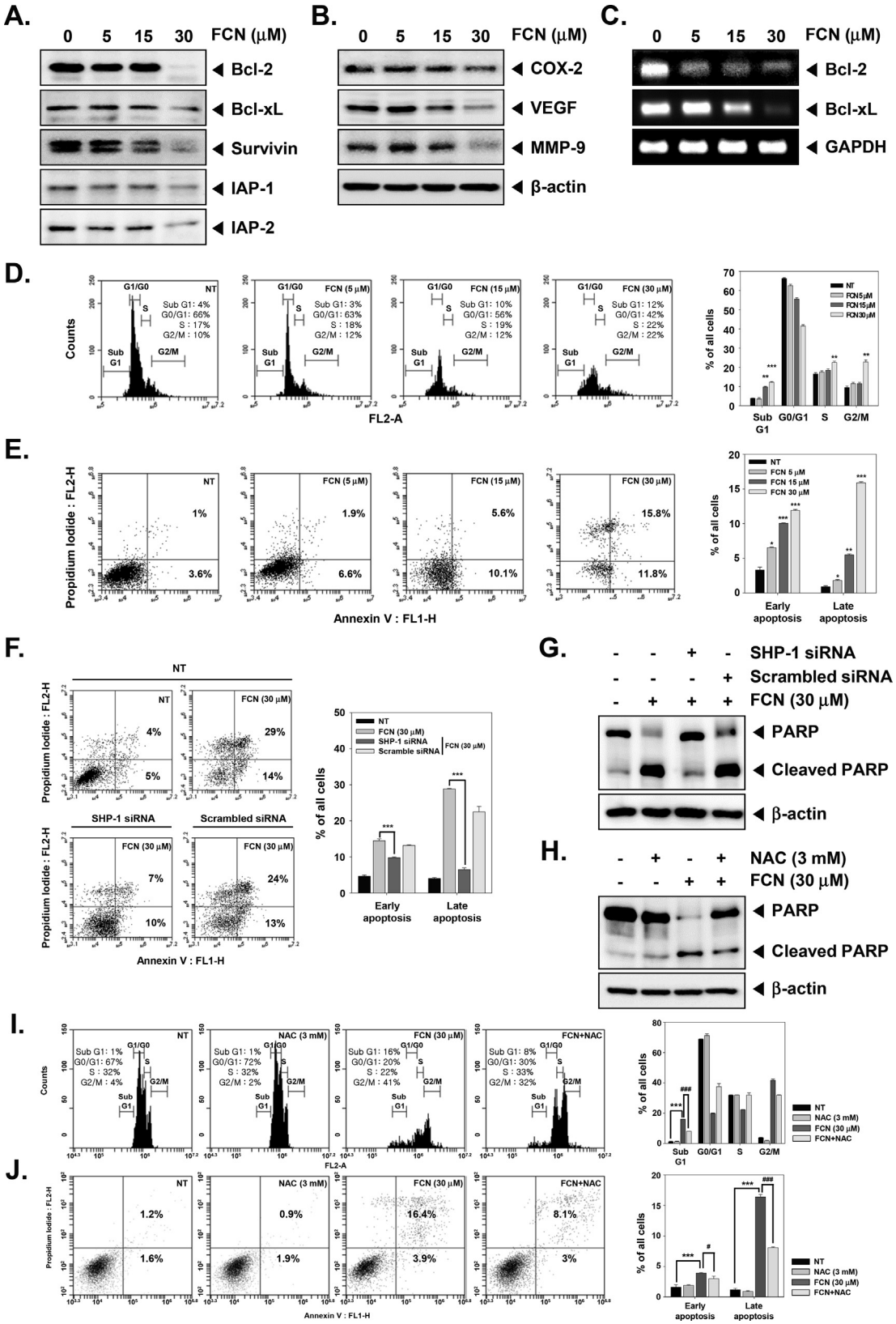

Fig. 4. ***FCN alters the levels of tumorigenic proteins.*** **(A and B)** U266 cells were treated with FCN for 24 h. Protein levels of various molecules were measured by Western blotting. **(C)** RNA levels of Bcl-2 and Bcl-xl was evaluated by reverse transcription PCR (RT-PCR). **(D-F)** U266 cells were treated with FCN and apoptotic cells were analyzed for cell cycle distribution, Annexin V and TUNEL assays using by BD Accuri™ C6 Plus Flow Cytometer. **(G)** U266 cells were transfected with SHP-1 siRNA, and treated with FCN (30 μM) for 24 h and western blotting was executed **(H)** U266 cells were pre-treated with NAC (3 mM) for 15 min, and then exposed to FCN for 24 h. Apoptosis was evaluated my measuring protein activation by Western blotting. (I-J) U266 cells were pre-treated with NAC (3 mM) for 15 min, and treated by FCN (30 μM) for 24 h. Apoptotic cells were analyzed by cell cycle assay and annexin V assay with BD Accuri™ C6 Plus Flow Cytometer. ### $p < 0.001$ vs. FCN + NAC treated cells, # $p < 0.05$ vs. FCN + NAC treated cells, and *** $p < 0.001$ vs. non-treated (NT) cells.

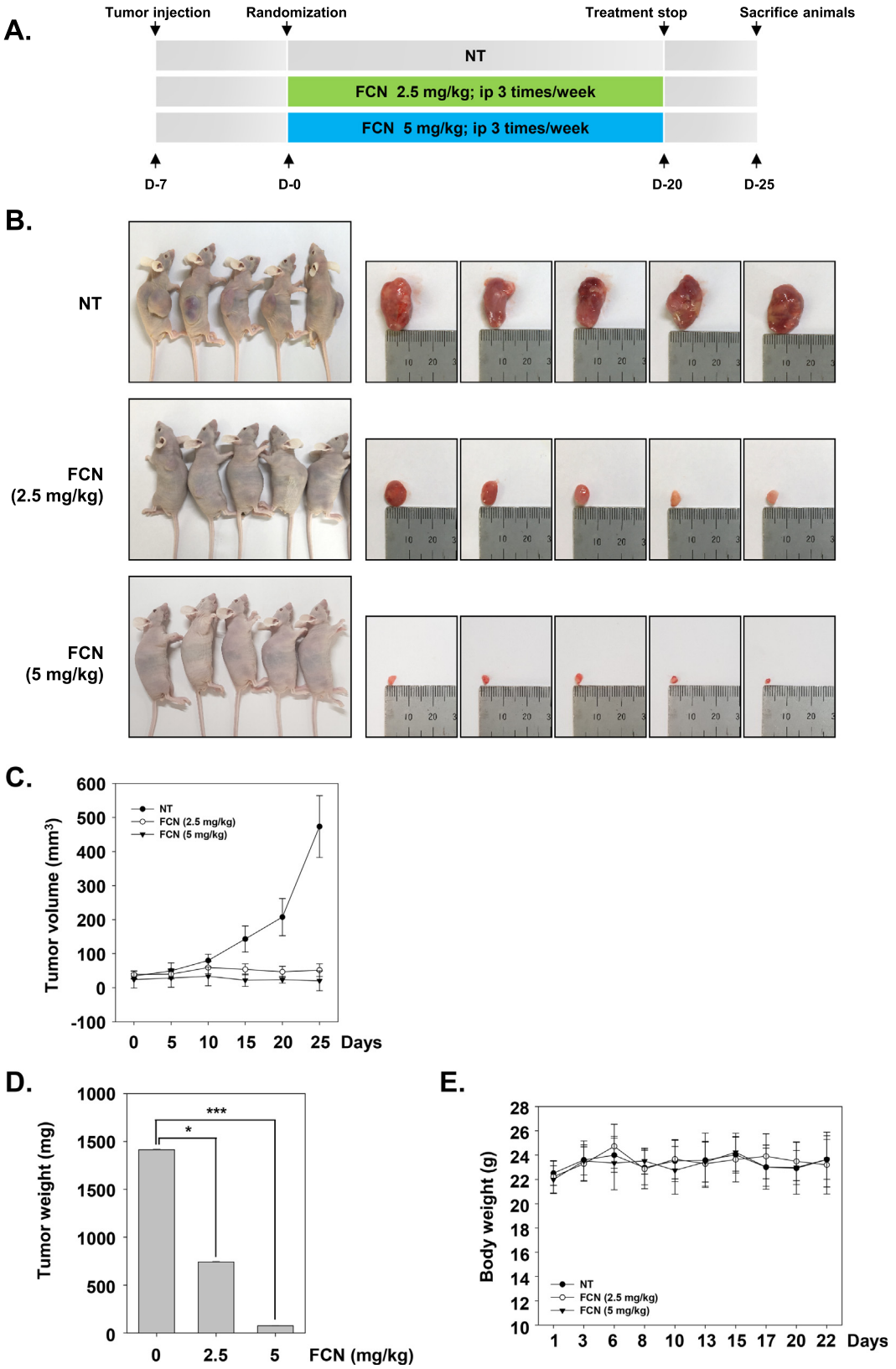

Fig. 5. ***Effects of FCN on tumorigenesis inhibition in myeloma xenograft model.*** **(A)** A depiction of *in vivo* experimental protocol. **(B)** Necropsy photographs of tumors at day 25. **(C)** Tumor volume was noted every 5 days (mean ± SE). **(D)** Tumor weight was analyzed on day 25, the last day of the experiment (mean ± SE). **(E)** Body weight was measured on the indicated days.

expression was confirmed. The results suggested that FCN exerted promising anticancer activities not only in tumor cells but also in preclinical settings, and can compensate for weight loss, a typical side effect noticed with existing anticancer drugs.

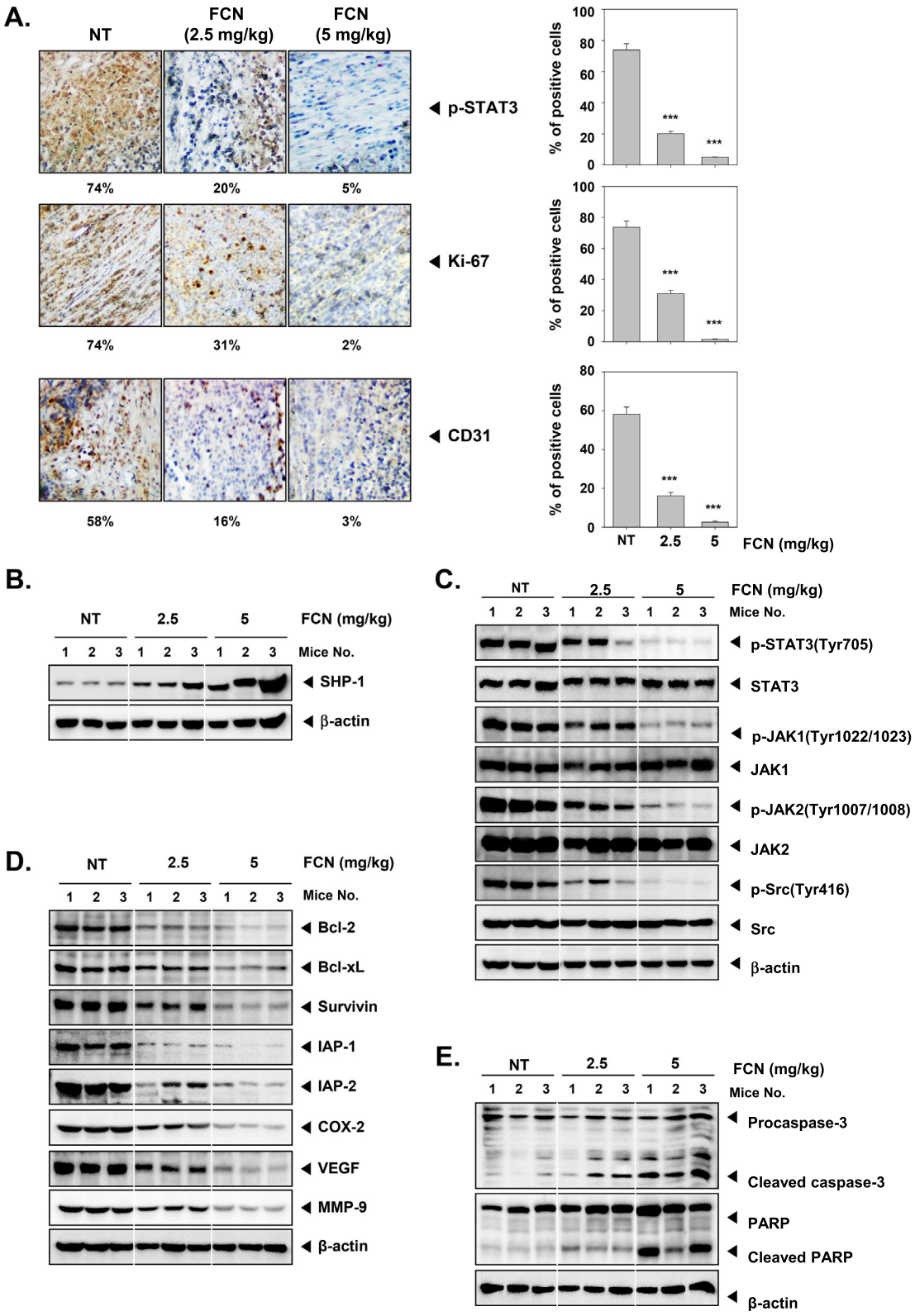

Fig. 6. ***Suppressive actions of FCN on proliferation, survival, and angiogenesis in tumor tissues.*** **(A)** Tumor tissues were obtained from FCN treated mice were studied by immunohistochemical analysis for various markers. **(B)** Western blot analysis with tissues samples for SHP-1 protein. **(C)** Western blot analysis to analyze the phosphorylation of STAT3 and upstream kinases. **(D)** Western blot to determine the levels of tumorigenic proteins. **(E)**. Western blot to measure the levels of apoptotic proteins.

Overall, our study clearly demonstrates for the first time a potential impact of FCN on STAT3 activation cascade that can be applied as a possible future therapy against diverse human cancers. Furthermore, FCN induced its multifaceted anti-cancer effects by altering oxidative stress, inducing SHP-1 levels and causing apoptosis. The alteration of redox status induced by FCN appear

to contribute substantially to its STAT3 suppressive actions and induction of apoptosis. Thus, this study suggests the possibility of developing novel pharmacological strategies using anti-neoplastic potential of FCN.

Funding

This work was supported by a National Research Foundation of Korea (NRF) grant funded by the Korean government (MSIP) (NRF-2018R1D1A1B07042969).

Compliance with Ethics Requirements

All Institutional and National Guidelines for the care and use of animals (fisheries) were followed.

CRediT authorship contribution statement

Young Yun Jung: Data curation, Formal analysis. **In Jin Ha:** Data curation, Formal analysis. **Jae-Young Um:** Formal analysis, Supervision. **Gautam Sethi:** Supervision, Writing - original draft. **Kwang Seok Ahn:** Supervision, Writing - original draft.

Declaration of Competing Interest

The authors declare that they have no known competing financial interests or personal relationships that could have appeared to influence the work reported in this paper.

Appendix A. Supplementary material

Supplementary data to this article can be found online at https://doi.org/10.1016/j.jare.2021.03.008.

References

[1] Baek SH, Lee JH, Kim C, Ko JH, Ryu SH, Lee SG, et al. Ginkgolic Acid C 17:1, derived from ginkgo biloba leaves, suppresses constitutive and inducible STAT3 Activation through induction of PTEN and SHP-1 tyrosine phosphatase. Molecules 2017;22(2).
[2] Lee JH, Kim C, Ko JH, Jung YY, Jung SH, Kim E, et al. Casticin inhibits growth and enhances ionizing radiation-induced apoptosis through the suppression of STAT3 signaling cascade. J Cell Biochem 2019;120(6):9787–98.
[3] Jung YY, Lee JH, Nam D, Narula AS, Namjoshi OA, Blough BE, et al. Anti-myeloma effects of icariin are mediated through the attenuation of JAK/STAT3-dependent signaling cascade. Front Pharmacol 2018;9:531.
[4] Lee M, Hirpara JL, Eu JQ, Sethi G, Wang L, Goh BC, et al. Targeting STAT3 and oxidative phosphorylation in oncogene-addicted tumors. Redox Biol 2019;25:101073.
[5] Zhang J, Ahn KS, Kim C, Shanmugam MK, Siveen KS, Arfuso F, et al. Nimbolide-induced oxidative stress abrogates STAT3 signaling cascade and inhibits tumor growth in transgenic adenocarcinoma of mouse prostate model. Antioxid Redox Signal 2016;24(11):575–89.
[6] Li F, Shanmugam MK, Chen L, Chatterjee S, Basha J, Kumar AP, et al. Garcinol, a polyisoprenylated benzophenone modulates multiple proinflammatory signaling cascades leading to the suppression of growth and survival of head and neck carcinoma. Cancer Prev Res (Phila) 2013;6(8):843–54.
[7] Kim SM, Lee JH, Sethi G, Kim C, Baek SH, Nam D, et al. Bergamottin, a natural furanocoumarin obtained from grapefruit juice induces chemosensitization and apoptosis through the inhibition of STAT3 signaling pathway in tumor cells. Cancer Lett 2014;354(1):153–63.
[8] Baek SH, Ko JH, Lee H, Jung J, Kong M, Lee JW, et al. Resveratrol inhibits STAT3 signaling pathway through the induction of SOCS-1: role in apoptosis induction and radiosensitization in head and neck tumor cells. Phytomedicine 2016;23(5):566–77.
[9] Han Y, Amin HM, Franko B, Frantz C, Shi X, Lai R. Loss of SHP1 enhances JAK3/STAT3 signaling and decreases proteosome degradation of JAK3 and NPM-ALK in ALK+ anaplastic large-cell lymphoma. Blood 2006;108(8):2796–803.
[10] Kim C, Cho SK, Kapoor S, Kumar A, Vali S, Abbasi T, et al. beta-Caryophyllene oxide inhibits constitutive and inducible STAT3 signaling pathway through induction of the SHP-1 protein tyrosine phosphatase. Mol Carcinog 2014;53(10):793–806.
[11] Lee JH, Chiang SY, Nam D, Chung WS, Lee J, Na YS, et al. Capillarisin inhibits constitutive and inducible STAT3 activation through induction of SHP-1 and SHP-2 tyrosine phosphatases. Cancer Lett 2014;345(1):140–8.
[12] Mohan CD, Rangappa S, Preetham HD, Chandra Nayaka S, Gupta VK, Basappa S, et al. Targeting STAT3 signaling pathway in cancer by agents derived from Mother Nature. Semin Cancer Biol 2020.
[13] Loh CY, Arya A, Naema AF, Wong WF, Sethi G, Looi CY. Signal transducer and activator of transcription (STATs) proteins in cancer and inflammation: functions and therapeutic implication. Front Oncol 2019;9:48.
[14] Arora L, Kumar AP, Arfuso F, Chng WJ, Sethi G. The role of signal transducer and activator of transcription 3 (STAT3) and its targeted inhibition in hematological malignancies. Cancers (Basel) 2018;10(9).
[15] Kerr JF, Wyllie AH, Currie AR. Apoptosis: a basic biological phenomenon with wide-ranging implications in tissue kinetics. Br J Cancer 1972;26(4):239–57.
[16] Wyllie AH, Kerr JF, Currie AR. Cell death: the significance of apoptosis. Int Rev Cytol 1980;68:251–306.
[17] Cryns V, Yuan J. Proteases to die for. Genes Dev 1998;12(11):1551–70.
[18] Los M, Wesselborg S, Schulze-Osthoff K. The role of caspases in development, immunity, and apoptotic signal transduction: lessons from knockout mice. Immunity 1999;10(6):629–39.
[19] Cohen GM. Caspases: the executioners of apoptosis. Biochem J 1997;326(Pt 1):1–16.
[20] Lazebnik YA, Kaufmann SH, Desnoyers S, Poirier GG, Earnshaw WC. Cleavage of poly(ADP-ribose) polymerase by a proteinase with properties like ICE. Nature 1994;371(6495):346–7.
[21] Los M, Herr I, Friesen C, Fulda S, Schulze-Osthoff K, Debatin KM. Cross-resistance of CD95- and drug-induced apoptosis as a consequence of deficient activation of caspases (ICE/Ced-3 proteases). Blood 1997;90(8):3118–29.
[22] Kaufmann SH, Desnoyers S, Ottaviano Y, Davidson NE, Poirier GG. Specific proteolytic cleavage of poly(ADP-ribose) polymerase: an early marker of chemotherapy-induced apoptosis. Cancer Res 1993;53(17):3976–85.
[23] Nicholson DW, Ali A, Thornberry NA, Vaillancourt JP, Ding CK, Gallant M, et al. Identification and inhibition of the ICE/CED-3 protease necessary for mammalian apoptosis. Nature 1995;376(6535):37–43.
[24] Merarchi M, Sethi G, Fan L, Mishra S, Arfuso F, Ahn KS. Molecular targets modulated by fangchinoline in tumor cells and preclinical models. Molecules 2018;23(10).
[25] Cilloni D, Martinelli G, Messa F, Baccarani M, Saglio G. Nuclear factor kB as a target for new drug development in myeloid malignancies. Haematologica 2007;92(9):1224–9.
[26] Fabricant DS, Farnsworth NR. The value of plants used in traditional medicine for drug discovery. Environ Health Perspect 2001;109(Suppl 1):69–75.
[27] Wang CD, Yuan CF, Bu YQ, Wu XM, Wan JY, Zhang L, et al. Fangchinoline inhibits cell proliferation via Akt/GSK-3beta/ cyclin D1 signaling and induces apoptosis in MDA-MB-231 breast cancer cells. Asian Pac J Cancer Prev 2014;15(2):769–73.
[28] Wang C, Kar S, Lai X, Cai W, Arfuso F, Sethi G, et al. Triple negative breast cancer in Asia: an insider's view. Cancer Treat Rev 2018;62:29–38.
[29] Xing Z, Zhang Y, Zhang X, Yang Y, Ma Y, Pang D. Fangchinoline induces G1 arrest in breast cancer cells through cell-cycle regulation. Phytother Res 2013;27(12):1790–4.
[30] Jung YY, Shanmugam MK, Chinnathambi A, Alharbi SA, Shair OHM, Um JY, et al. Fangchinoline, a bisbenzylisoquinoline alkaloid can modulate cytokine-impelled apoptosis via the dual regulation of NF-kappaB and AP-1 pathways. Molecules 2019;24(17).
[31] Li X, Yang Z, Han W, Lu X, Jin S, Yang W, et al. Fangchinoline suppresses the proliferation, invasion and tumorigenesis of human osteosarcoma cells through the inhibition of PI3K and downstream signaling pathways. Int J Mol Med 2017;40(2):311–8.
[32] Guo B, Su J, Zhang T, Wang K, Li X. Fangchinoline as a kinase inhibitor targets FAK and suppresses FAK-mediated signaling pathway in A549. J Drug Target 2015;23(3):266–74.
[33] Shi J, Guo B, Hui Q, Chang P, Tao K. Fangchinoline suppresses growth and metastasis of melanoma cells by inhibiting the phosphorylation of FAK. Oncol Rep 2017;38(1):63–70.
[34] Klaunig JE. Oxidative stress and cancer. Curr Pharm Des 2018;24(40):4771–8.
[35] Moloney JN, Cotter TG. ROS signalling in the biology of cancer. Semin Cell Dev Biol 2018;80:50–64.
[36] Peng B, Xu L, Cao F, Wei T, Yang C, Uzan G, et al. HSP90 inhibitor, celastrol, arrests human monocytic leukemia cell U937 at G0/G1 in thiol-containing agents reversible way. Mol Cancer 2010;9:79.
[37] Lee JH, Kim C, Lee SG, Sethi G, Ahn KS. Ophiopogonin D, a steroidal glycoside abrogates STAT3 signaling cascade and exhibits anti-cancer activity by causing GSH/GSSG imbalance in lung carcinoma. Cancers (Basel) 2018;10(11).
[38] Kirtonia A, Sethi G, Garg M. The multifaceted role of reactive oxygen species in tumorigenesis. Cell Mol Life Sci 2020.
[39] Zukowski P, Maciejczyk M, Matczuk J, Kurek K, Waszkiel D, Zendzian-Piotrowska M, et al. Effect of N-acetylcysteine on antioxidant defense, oxidative modification, and salivary gland function in a rat model of insulin resistance. Oxid Med Cell Longev 2018;2018:6581970.
[40] Flohe L. The fairytale of the GSSG/GSH redox potential. Biochim Biophys Acta 2013;1830(5):3139–42.
[41] Deponte M. Glutathione catalysis and the reaction mechanisms of glutathione-dependent enzymes. Biochim Biophys Acta 2013;1830(5):3217–66.
[42] Hwang ST, Kim C, Lee JH, Chinnathambi A, Alharbi SA, Shair OHM, et al. Cycloastragenol can negate constitutive STAT3 activation and promote

paclitaxel-induced apoptosis in human gastric cancer cells. Phytomedicine 2019;59:152907.
[43] Kim C, Lee SG, Yang WM, Arfuso F, Um JY, Kumar AP, et al. Formononetin-induced oxidative stress abrogates the activation of STAT3/5 signaling axis and suppresses the tumor growth in multiple myeloma preclinical model. Cancer Lett 2018;431:123–41.
[44] Mahbub AA, Le Maitre CL, Haywood-Small SL, Cross NA, Jordan-Mahy N. Polyphenols act synergistically with doxorubicin and etoposide in leukaemia cell lines. Cell Death Discov 2015;1:15043.
[45] Jung YY, Shanmugam MK, Narula AS, Kim C, Lee JH, Namjoshi OA, et al. Oxymatrine attenuates tumor growth and deactivates STAT5 signaling in a lung cancer xenograft model. Cancers (Basel) 2019;11(1).
[46] Lee JH, Kim C, Sethi G, Ahn KS. Brassinin inhibits STAT3 signaling pathway through modulation of PIAS-3 and SOCS-3 expression and sensitizes human lung cancer xenograft in nude mice to paclitaxel. Oncotarget 2015;6(8):6386–405.
[47] Sakamuru S, Attene-Ramos MS, Xia M. Mitochondrial membrane potential assay. Methods Mol Biol 2016;1473:17–22.
[48] Krifka S, Hiller KA, Spagnuolo G, Jewett A, Schmalz G, Schweikl H. The influence of glutathione on redox regulation by antioxidant proteins and apoptosis in macrophages exposed to 2-hydroxyethyl methacrylate (HEMA). Biomaterials 2012;33(21):5177–86.